Highly Anisotropic and Twofold Symmetric Superconducting Gap in Nematically Ordered $FeSe_{0.93}S_{0.07}$

H. C. Xu,[1] X. H. Niu,[1] D. F. Xu,[1] J. Jiang,[1] Q. Yao,[1] Q. Y. Chen,[1] Q. Song,[1] M. Abdel-Hafiez,[2,3] D. A. Chareev,[4,5] A. N. Vasiliev,[5,6] Q. S. Wang,[1] H. L. Wo,[1] J. Zhao,[1] R. Peng,[1,*] and D. L. Feng[1,†]

[1]*State Key Laboratory of Surface Physics, Department of Physics, and Advanced Materials Laboratory, Fudan University, Shanghai 200433, People's Republic of China*

[2]*Center for High Pressure Science and Technology Advanced Research, Beijing 100094, China*

[3]*Faculty of science, Physics Department, Fayoum University, 63514 Fayoum, Egypt*

[4]*Institute of Experimental Mineralogy, Russian Academy of Sciences, 142432 Chernogolovka, Moscow District, Russia*

[5]*Institute of Physics and Technology, Ural Federal University, 620002 Ekaterinburg, Russia*

[6]*Low Temperature Physics and Superconductivity Department, M.V. Lomonosov Moscow State University, 119991 Moscow, Russia*

(Received 26 March 2016; revised manuscript received 10 July 2016; published 7 October 2016)

FeSe exhibits a novel ground state in which superconductivity coexists with a nematic order in the absence of any long-range magnetic order. Here, we report on an angle-resolved photoemission study on the superconducting gap structure in the nematic state of $FeSe_{0.93}S_{0.07}$, without the complications caused by Fermi surface reconstruction induced by magnetic order. We find that the superconducting gap shows a pronounced twofold anisotropy around the elliptical hole pocket near Z (0, 0, π), with gap minima at the end points of its major axis, while no detectable gap is observed around Γ (0, 0, 0) and the zone corner (π, π, k_z). The large anisotropy and nodal gap distribution demonstrate the substantial effects of the nematicity on the superconductivity and thus put strong constraints on current theories.

DOI: 10.1103/PhysRevLett.117.157003

The pairing mechanism underlying unconventional superconductivity is often related to the quantum fluctuations of nearby orders. In most Fe-based superconductors, both magnetic and nematic orders appear simultaneously near the superconducting state. These orders are believed to play critical roles in the superconductivity, and both spin-fluctuation-mediated and orbital-fluctuation-mediated superconducting pairing mechanisms have been proposed [1–5]. Although intense experimental studies have been conducted [6–13], the roles of spin and orbital degrees of freedom and the exact pairing mechanism in Fe-based superconductors are still under heated debate.

FeSe is a unique material with a novel superconducting state. Orbital order develops in the nematic state of FeSe without breaking the translational symmetry in angle-resolved photoemission spectroscopy (ARPES) studies [14,15]. The superconductivity coexists with the nematic order without any long-range magnetic order [16], thus disentangling the magnetic and orbital orders. Moreover, recent results suggest that FeSe is a quantum paramagnet [4] with coexisting Néel and stripe antiferromagnetic interactions [17,18]. The novel ground state in FeSe provides a fresh perspective for studying the effects of nematic order on the superconducting gap structure in the absence of the Fermi surface reconstruction induced by magnetic order, which helps to reveal the roles of spin and orbital degrees of freedom in unconventional superconductivity. The superconducting gap structure of FeSe and $FeSe_{1-x}S_x$ has been under intensive debate, while no consensus has been reached on whether there are nodes [19–21] or whether it has a nodeless multigap structure [22–29]. Besides, although the vortex elongation in scanning tunneling spectroscopy (STS) suggests possible twofold gap symmetry [19,21], the band- and momentum-resolved gap structure is still unknown. ARPES studies on the superconducting gap structure of $FeSe/FeSe_{1-x}S_x$ is lacking due to the low T_c and small gap size.

In this work, we studied the superconducting gap structure of $FeSe_{0.93}S_{0.07}$ single crystals ($T_c \sim 9.8$ K) [29,30] by ARPES. At 6.3 K, both the nematic electronic structure and the superconducting gap are resolved. The maximal gap at the hole pocket is ~2.5 meV, similar to that measured by STS [21]. The superconducting gap shows twofold anisotropy around the Z point (0, 0, π), and it is undetectable around the hole pocket near Γ (0, 0, 0) and the electron pockets at the zone corners (π, π, k_z). These findings help to examine the previous controversial gap structures deduced from STS and thermodynamics measurements. The unique gap structure observed here cannot be reasonably fitted by most of the known theoretical

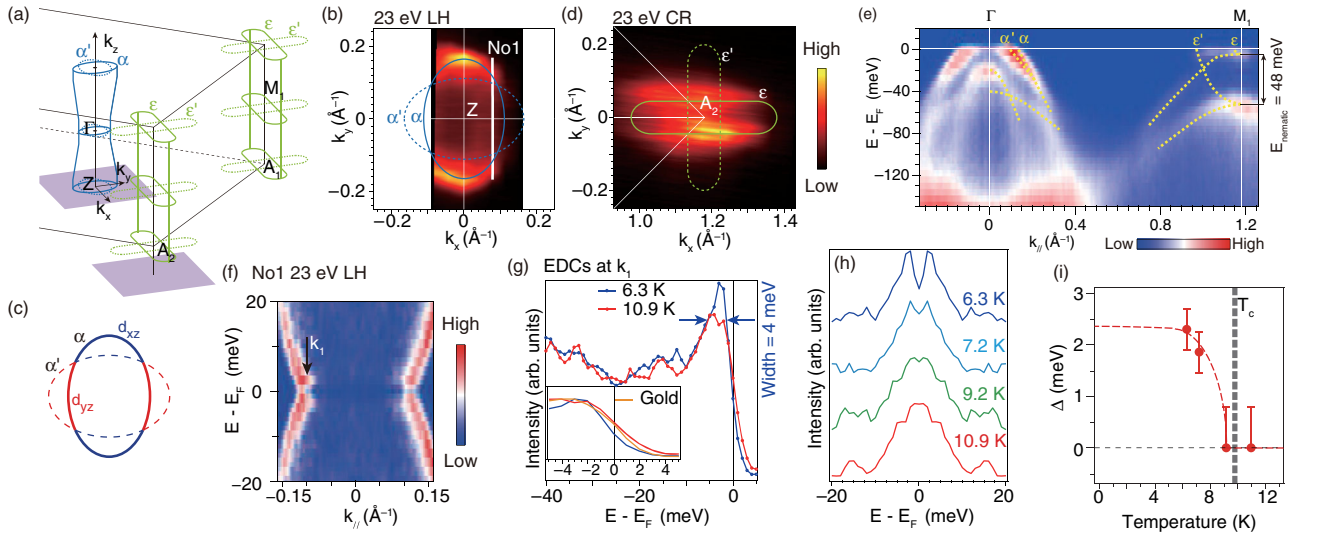

FIG. 1. (a) Fermi surfaces in the two-Fe Brillouin zone of FeSe in the nematic state measured by ARPES [36]. (b) Fermi surface mapping around Z with linear-horizontal (LH) polarized photons. The corresponding momenta are indicated by the purple square in (a). (c) Orbital character of pocket α (the solid ellipse) and its counterpart from twin domains (α', the dashed ellipse). (d) Same as (b), but around A_2 with circular-right (CR) polarized photons. (e) Photoemission intensity along $\Gamma - M_1$. E_{nematic} indicates the band splitting due to nematic ordering. (f) Symmetrized photoemission intensity along cut No1, as indicated in (c). (g) Energy distribution curves (EDCs) above and below T_c at the momentum k_1 in (f). The width of the superconducting quasiparticle peak is indicated. (Inset) The leading edge shift resulting from the gap opening. (h) Temperature dependent symmetrized EDCs at the momentum k_1. (i) Superconducting gap size as a function of temperature fits to the Bardeen-Cooper-Schrieffer formula.

models and their simple combinations, which suggests that the effects of nematicity on the superconductivity are substantial.

$FeSe_{0.93}S_{0.07}$ single crystals were grown using $AlCl_3/KCl$ flux in a temperature gradient (from 400 °C to 350 °C) for 45 days [29,31]. Electron probe microanalysis (EPMA) measurements give the chemical composition $Fe(Se_{0.926\pm0.016}S_{0.074\pm0.007})_{0.94}$ [32]. The ARPES measurements were conducted at beam line I05 of the Diamond Light Source and beam line 5-4 of the Stanford Synchrotron Radiation Lightsource (SSRL). The data were taken at the temperature of 6.3 K unless otherwise specified. The single crystals were cleaved *in situ* and measured under ultrahigh vacuum better than 1×10^{-10} mbar. For data collection with 23 eV (37 eV) photons, the energy resolution was 3 meV (5 meV), unless otherwise specified. This allows for resolving a superconducting gap of 0.8 meV (1.6 meV) [32,33].

As illustrated in Fig. 1(a), the Fermi surfaces of $FeSe/FeSe_{1-x}S_x$ in the nematic state measured by ARPES generally consist of two hole pockets (α and α') around the zone center and two electron pockets (ε and ε') around the zone corner [14,34–36]. α and α' are equivalent since the latter comes from the 90°-rotated twin domains [14,34,36]. The two electron pockets ε and ε' are perpendicular to each other. They could be perpendicular due to the twinning (plotted in the way here), each from one of the two 90°-rotated twin domains [14,34,36]; alternatively, they could both be from the same domain, as suggested in a recent ARPES study [37]. In our data, the elliptical hole pockets α and α' and the elongated electron pockets ε and ε' are resolved [Figs. 1(b) and 1(d)]. The spectral weight distribution under the linear polarization suggests mixed d_{xz} and d_{yz} orbitals in both α and α' pockets [Fig. 1(c)] [32,38], consistent with the previous ARPES study on FeSe [14]. The nematic splitting between bands ε and ε' at M is 48 meV [Fig. 1(e)], which agrees with a previous report on $FeSe_{1-x}S_x$ [34], indicating that the nematicity is slightly suppressed compared to FeSe but is still strong.

At 6.3 K, band α shows a gap and a back-bending dispersion [Fig. 1(f)], which are the hallmarks of Bogoliubov quasiparticles. Sharp quasiparticle peaks are observed at the Fermi crossings of band α at 10.9 K, and they become even sharper at 6.3 K [Fig. 1(g)]. Since quasiparticle peaks in ARPES spectra could easily be broadened or destroyed by disorder scattering [39], the resolution-limited width of the coherent peak here indicates the low defect density and the high quality of the sample. From 10.9 to 6.3 K, the leading edge shifts below the Fermi energy [see the inset of Fig. 1(g)], indicating a gap opening. The gap size determined by the symmetrized energy distribution curves (EDCs) is around 2.5 meV at 6.3 K [Fig. 1(h)], which decreases with increasing temperature and eventually closes at around 9.2 K [32], following the Bardeen-Cooper-Schrieffer formula [Fig. 1(i)]. The gap closing temperature is close to the $T_c \sim 9.8$ K value measured by transport experiments [29], indicating the superconducting nature of the observed gap.

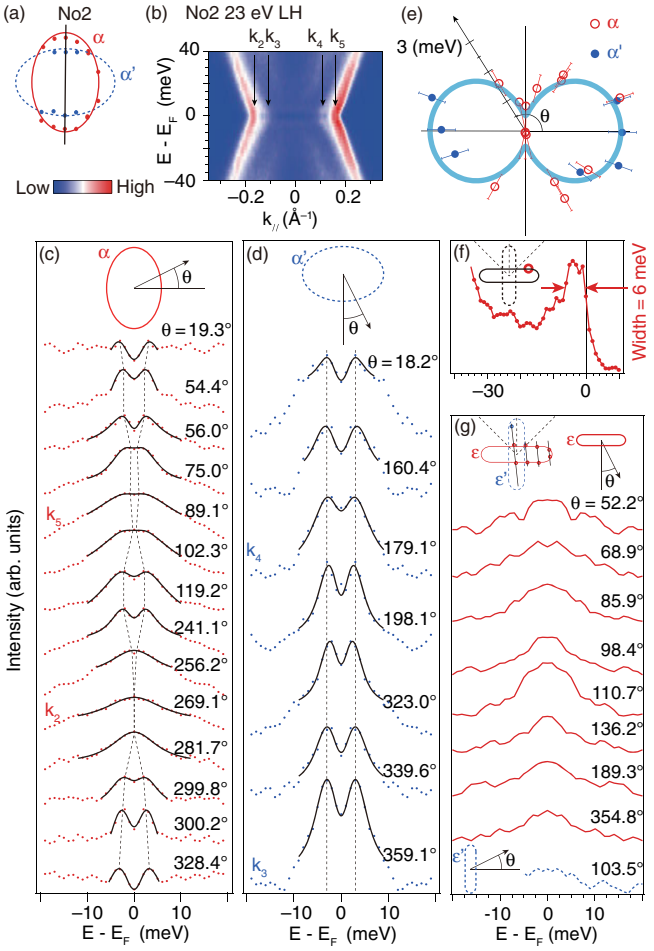

FIG. 2. (a) Illustration of hole pockets α and α' around the Z point. (b) Symmetrized photoemission intensity along cut No2, as indicated in (a). (c) Symmetrized EDCs (the red dots) on the pocket α, and superconducting spectra (the black curves) obtained following the standard fitting procedure [32,33,40]. The insets define the in-plane angle θ. (d) Symmetrized EDCs (the blue dots) on the pocket α' and fitted superconducting spectra (the black curves). (e) Polar plot of the superconducting gap as a function of θ along the pockets α and α'. (f) EDC at the pocket ε indicated by the red circle. (g) Symmetrized EDCs on the electron pockets ε (the red solid curves) and ε' (the blue dashed curve) around the A_1 point.

The momentum distribution of the superconducting gap on the hole pockets α and α' has been studied with 23 eV photons [Fig. 2(a)]. In the symmetrized photoemission intensity along cut No2, α' is gapped at momenta k_3 and k_4, whereas α crosses the Fermi level at momenta k_2 and k_5 without any observable gap opening [Fig. 2(b)], indicating distinct gap sizes between the major-axis end points of pocket α and the minor axis end points of pocket α'. As shown by the symmetrized EDCs in Fig. 2(c), the superconducting gap is reduced around the major-axis end points of the elliptical Fermi surface α ($\theta \simeq 90°$ and 270°). Around the minor axis end points of pocket α', the gap size remains constant [see Fig. 2(d) and the Supplemental Material [32]]. By empirically fitting to a superconducting spectral function [Figs. 2(c) and 2(d)] [32,33,40], the sizes of the superconducting gap as a function of the polar angle θ are summarized in one single polar plot [Fig. 2(e)], noting that α and α' are identical bands from twin domains. The superconducting gap on band α shows anisotropy with twofold symmetry. The gap size decreases from about 2.5 meV at the minor axis end points of the ellipse to less than 0.8 meV around the major-axis end points, which is at the experimental resolution limit. The maximum gap size of ~2.5 meV is similar to the gap maximum of 2.6 meV of $FeSe_{0.93}S_{0.04}$ [21] and slightly larger than the 2.2 meV of FeSe [19] measured by STS.

The photoemission spectra at the Fermi crossing of band ε show sharp quasiparticle peaks in the superconducting state [Fig. 2(f)]. However, no superconducting gap is detected on the electron pockets ε or ε' at different k_z's [see Fig. 2(g) and the Supplemental Material [32]]. The absence of a superconducting gap at these momenta indicates nodes or a small gap size below the experimental resolution limit.

At 37 eV photon energy, the bands α and α' are resolved along cut No3 [Fig. 3(b)], showing sharp quasiparticle peaks at the Fermi crossings [Fig. 3(c)]. Along the elliptical Fermi surface α', the symmetrized EDCs show no detectable superconducting gaps [Fig. 3(d)], indicating nodes or a small gap size below the experimental resolution limit. For band α, the Fermi crossings with polar angles 264.0° and 275.0° show no observable gap either [Fig. 3(e)]. The quasiparticle peaks at $\sim \pm 4$ meV for $\theta = 80.6°$ and 95.0° are contributed by band α', which gives false signatures of the gap opening in Fig. 3(e). Actually, as shown in Figs. 3(f) and 3(g), the EDCs divided by the resolution-convolved Fermi-Dirac function are flat within 2 to 3 meV of the Fermi crossings of band α, indicating no detectable gap opening. As shown in the Supplemental Material [32], the gap amplitude decreases from Z to Γ and eventually diminishes, which is intriguingly opposite to the amplitudes observed in $BaFe_2(As_{1-x}P_x)_2$ and $Ba_{1-x}K_xFe_2As_2$ [33,41], where the gap of the α band increases from Z to Γ.

Our momentum-resolved data show the profound gap anisotropy at the hole pocket, and the gap size at the electron pocket is negligible, if not zero. The twofold anisotropy of the gap is consistent with the twofold symmetric vortex observed in the STS studies on $FeSe_{1-x}S_x$ [19,21]. Our results also agree with the V-shaped gap in the STS studies [19,21,26] and the large gap anisotropy deduced from fittings of specific heat and London penetration depth data [20,22,27,28]. However, our observations cannot be accounted for by some fittings of specific heat and London penetration depth that give two gaps with similar sizes [29], or theories with isotropic gap at the hole pocket [42]. Because of the lack of momentum-resolved knowledge on the gap, some thermodynamic data

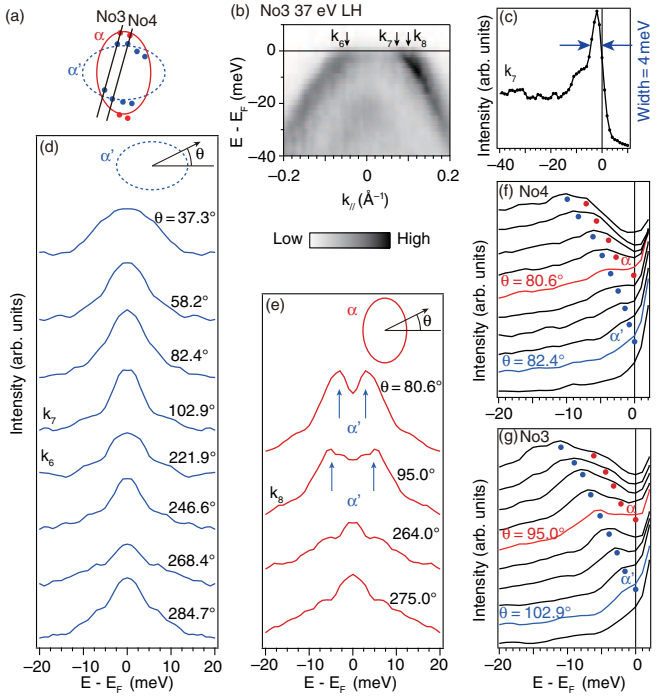

FIG. 3. (a) Illustration of pockets α and α' around the Γ point. (b) Photoemission intensity along cut No3, as indicated in (a). (c) The EDC at momentum k_7. (d) Symmetrized EDCs on the pocket α'. The inset defines the in-plane angle θ. (e) Symmetrized EDCs on the pocket α. Quasiparticle peaks from band α' are indicated. (f) EDCs divided by the resolution-convolved Fermi-Dirac function near the upper Fermi crossings of cut No4 in (a). (g) Same as (f) but near the upper Fermi crossings of cut No3.

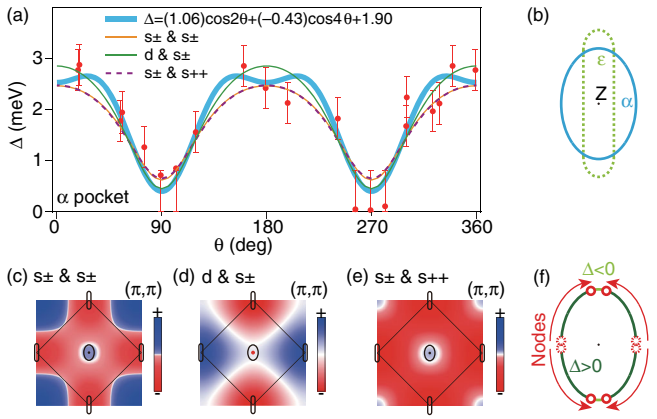

FIG. 4. (a) Angular dependence of the superconducting gap on the α pocket and fitting results by cosine series, $\Delta_{s\pm,s\pm}$, $\Delta_{d,s\pm}$, and $\Delta_{s\pm,s++}$. (b) Overlapping of the pockets ε (the dashed curves) and α (the solid curves) in the case of antiferromagnetic folding. (c)–(e) The gap forms obtained by the fitting results in (a). (f) The gap structure on the pocket α according to the theory of Ref. [46].

were fitted assuming that the electron pocket shows a larger gap than the hole pocket, and the gap anisotropy is fourfold or eightfold symmetric [22,25]. It is thus necessary to examine those data again based on the momentum-resolved gap information obtained here.

To investigate the origin of the novel gap structure in $FeSe_{0.93}S_{0.07}$, we first scrutinize four scenarios that do not consider nematicity.

First, in superconductivity with a dominant $s{+}{+}$ pairing mediated by orbital fluctuations, the gap form of a system without orbital ordering is nearly isotropic and nodeless [5], which is inconsistent with our observations.

Second, in an $s\pm$ pairing mediated by magnetic interactions, the sign-changing gap form may lead to gap anisotropy and nodes [43,44]. Since both Néel and stripe spin fluctuations exist in FeSe [18], if the $s\pm$ superconducting pairing were generated by either the (π, π) interaction with the gap form $\cos k_x \cos k_y$ or the $(\pi, 0)$ interaction with the gap form $(\cos k_x + \cos k_y)/2$ [44], the anisotropy of the superconducting gap on the elliptical α pocket would be 3% or 6%, respectively. These cannot account for the large anisotropy of at least 68% observed in our data.

If there were static stripe antiferromagnetic order with a wave vector $(\pi, 0)$, the electron pockets would have been folded to the zone center and would intersect with the α pocket [Fig. 4(b)]. Gap nodes would emerge on the reconstructed Fermi surfaces, given a large value of the antiferromagnetic order parameter [45]. However, FeSe shows no static magnetic order and no band folding; thus, its gap anisotropy cannot be explained by this scenario.

Third, a composite form of superconducting pairing may arise from the quantum paramagnet ground state with Néel and stripe spin fluctuations [4,18]. In Fig. 4(a), we fit the gap anisotropy of the α pocket by [19]

$$\Delta_{s\pm,s\pm} = \Delta_1 \cos k_x \cos k_y + \Delta_2(\cos k_x + \cos k_y)/2,$$

which gives the superconducting gap sizes $\Delta_1 = -58.2 \pm 8.8$ meV and $\Delta_2 = 62.2 \pm 9.2$ meV for the $s\pm$ pairing mediated by the two kinds of spin fluctuations. Moreover, the combination of the Néel spin-fluctuation-mediated d-wave pairing and the stripe spin-fluctuation-mediated $s\pm$ pairing with the gap form

$$\Delta_{d,s\pm} = \Delta_d(\cos k_x - \cos k_y)/2 + \Delta_2(\cos k_x + \cos k_y)/2$$

also gives a good fitting with $\Delta_1 = 30.3 \pm 2.8$ meV and $\Delta_2 = 2.24 \pm 0.09$ meV [Fig. 4(a)]. Alternatively, by combining the spin-fluctuation-mediated $s\pm$ pairing and the orbital-fluctuation-mediated $s{+}{+}$ pairing [5], the gap anisotropy at pocket α can be fitted by

$$\Delta_{s\pm,s++} = \Delta_2(\cos k_x + \cos k_y)/2 + \Delta_s,$$

with $\Delta_2 = 32.8 \pm 4.8$ meV and $\Delta_s = -28.7 \pm 4.4$ meV for the $s\pm$ and $s{+}{+}$ pairings, respectively [Fig. 4(a)]. All three fittings contain gap amplitudes over 30 meV, which is inconsistent with the low T_c of FeSe. Moreover, the obtained gap forms would give a large gap at the ε pocket [Figs. 4(c)–4(e)], in contrast to the undetectable

superconducting gap in our data. Therefore, the large gap anisotropy on pocket α is not likely a result of these simple combinations of gap forms.

Fourth, in the theory of orbital-antiphase pairing, a pocket consisting of only d_{xz}/d_{yz} orbitals like the pocket α in FeSe [Fig. 1(c)] would show a nearly isotropic gap [47,48], which is inconsistent with our observations.

Now we consider models that include nematicity. Nematicity lifts the degeneracy of d_{xz}/d_{yz} orbitals and would lead to an orbital-dependent superconducting pairing. Indeed, a stronger superconducting pairing for the d_{yz} orbital is observed here as the d_{yz} orbital characters coincide with the gap maxima on the α pocket [Figs. 1(c) and 2(e)]. In a recently proposed spin-fluctuation-mediated pairing scenario, the orbital ordering may mix different pairing symmetries and give rise to two pairs of accidental nodes on each hole pocket [46]. The positions of the nodes depend on the splitting between the d_{xz} and d_{yz} orbitals, which was assumed to be 80 meV in Ref. [46], close to the nematicity induced splitting of 50 meV in $FeSe_{0.93}S_{0.07}$ [Fig. 1(e)]. In this scenario, if a pair of nodes are located near the major-axis end point of the α pocket due to strong nematicity [Fig. 4(f)], the gap would exhibit just one minimum at each end point in an experiment with limited momentum resolution, consistent with our findings. On the other hand, in a scenario based on orbital-fluctuation-mediated pairing [49], it has been argued that a similar gap anisotropy might arise from an anisotropic $s{+}{+}$ pairing dominated by the d_{yz} orbital in the nematic state.

In summary, we revealed the superconducting gap structure of $FeSe_{0.93}S_{0.07}$ under the effect of nematicity disentangled from magnetic order. The gap amplitude decreased from Z to Γ, until it was undetectable at Γ, which is intriguingly different from that of $BaFe_2(As_{1-x}P_x)_2$ showing a nodal ring around Z. Profound anisotropy of a superconducting gap with two-fold symmetry was directly observed on the hole pocket α, and the gap on the hole pocket was significantly larger than that on the electron pockets. Such momentum-resolved gap information would help the analysis on the specific heat and London penetration depth of $FeSe_{1-x}S_x$. The gap structure cannot be understood by current theories unless the effects of nematicity are considered. The substantial effects of nematicity on superconductivity observed in our results establish a benchmark for future theories of Fe-based superconductors, where the quantitative fitting to our results would hopefully distinguish the pictures of spin-fluctuation-mediated and orbital-fluctuation-mediated pairing scenarios and help to reveal the superconducting mechanism.

We gratefully acknowledge the experimental support from Moritz Hoesh, Pavel Dudin, and Timur Kim at Diamond Light Source, and Donghui Lu and Makoto Hashimoto at the SSRL. We thank Yan Zhang for the helpful discussions and for sharing his unpublished data of independent measurement, and Darren Peets, Jiangping Hu, Dung-Hai Lee, Andrey Chubukov, Rafael Fernandes, Jian Kang for the helpful discussions. We thank Xiaoping Shen and Chenhaoping Wen for conducting the EPMA measurements. This work is supported in part by the National Key R&D Program of Ministry of Science and Technology of China (Grant No. 2016YFA0300203), the Science and Technology Commission of Shanghai Municipality under Grants No. 15YF1401000 and No. 15ZR1402900, and the Act 211 Government of the Russian Federation, Agreement No. 02.A03.21.0006.

*pengrui@fudan.edu.cn
†dlfeng@fudan.edu.cn

[1] P. J. Hirschfeld, M. M. Korshunov, and I. I. Mazin, Rep. Prog. Phys. **74**, 124508 (2011).
[2] J. K. Glasbrenner, I. I. Mazin, H. O. Jeschke, P. J. Hirschfeld, R. M. Fernandes, and R. Valentí, Nat. Phys. **11**, 953 (2015).
[3] R. Yu and Q. Si, Phys. Rev. Lett. **115**, 116401 (2015).
[4] F. Wang, S. A. Kivelson, and D.-H. Lee, Nat. Phys. **11**, 959 (2015).
[5] H. Kontani and S. Onari, Phys. Rev. Lett. **104**, 157001 (2010).
[6] Y. Zhang *et al.*, Nat. Mater. **10**, 273 (2011).
[7] D. F. Liu *et al.*, Nat. Commun. **3**, 931 (2012).
[8] M. Xu *et al.*, Phys. Rev. B **85**, 220504 (2012).
[9] B. Zeng, B. Shen, G. F. Chen, J. B. He, D. M. Wang, C. H. Li, and H. H. Wen, Phys. Rev. B **83**, 144511 (2011).
[10] W. Yu, L. Ma, J. B. He, D. M. Wang, T. L. Xia, G. F. Chen, and W. Bao, Phys. Rev. Lett. **106**, 197001 (2011).
[11] J. T. Park *et al.*, Phys. Rev. Lett. **107**, 177005 (2011).
[12] R. Peng *et al.*, Phys. Rev. Lett. **112**, 107001 (2014).
[13] Q. Fan *et al.*, Nat. Phys. **11**, 946 (2015).
[14] M. D. Watson *et al.*, Phys. Rev. B **91**, 155106 (2015).
[15] Y. Zhang *et al.*, arXiv:1503.01556.
[16] T. M. McQueen, A. J. Williams, P. W. Stephens, J. Tao, Y. Zhu, V. Ksenofontov, F. Casper, C. Felser, and R. J. Cava, Phys. Rev. Lett. **103**, 057002 (2009).
[17] Q. Wang *et al.*, Nat. Mater. **15**, 159 (2016).
[18] Q. Wang *et al.*, Nat. Commun. **7**, 12182 (2016).
[19] C. L. Song *et al.*, Science **332**, 1410 (2011).
[20] S. Kasahara *et al.*, Proc. Natl. Acad. Sci. U.S.A. **111**, 16309 (2014).
[21] S. A. Moore, J. L. Curtis, C. Di Giorgio, E. Lechner, M. Abdel-Hafiez, O. S. Volkova, A. N. Vasiliev, D. A. Chareev, G. Karapetrov, and M. Iavarone, Phys. Rev. B **92**, 235113 (2015).
[22] J.-Y. Lin, Y. S. Hsieh, D. A. Chareev, A. N. Vasiliev, Y. Parsons, and H. D. Yang, Phys. Rev. B **84**, 220507 (2011).
[23] D. Chareev, E. Osadchii, T. Kuzmichev, J.-Y. Lin, S. Kuzmichev, O. Volkova, and A. Vasiliev, CrystEngComm **15**, 1989 (2013).
[24] J. K. Dong, T. Y. Guan, S. Y. Zhou, X. Qiu, L. Ding, C. Zhang, U. Patel, Z. L. Xiao, and S. Y. Li, Phys. Rev. B **80**, 024518 (2009).

[25] L. Jiao, C.-L. Huang, S. Rößler, C. Koz, U. K. Rößler, U. Schwarz, and S. Wirth, arXiv:1605.01908.
[26] P. Bourgeois-Hope, S. Chi, D. A. Bonn, R. Liang, W. N. Hardy, T. Wolf, C. Meingast, N. Doiron-Leyraud, and L. Taillefer, Phys. Rev. Lett. **117**, 097003 (2016).
[27] R. Khasanov *et al.*, Phys. Rev. B **78**, 220510 (2008).
[28] M. Abdel-Hafiez, J. Ge, A. N. Vasiliev, D. A. Chareev, J. Van de Vondel, V. V. Moshchalkov, and A. V. Silhanek, Phys. Rev. B **88**, 174512 (2013).
[29] M. Abdel-Hafiez *et al.*, Phys. Rev. B **91**, 165109 (2015).
[30] M. Abdel-Hafiez, Y. J. Pu, J. Brisbois, R. Peng, D. L. Feng, D. A. Chareev, A. V. Silhanek, C. Krellner, A. N. Vasiliev, and X.-J. Chen, Phys. Rev. B **93**, 224508 (2016).
[31] D. Chareev, E. Osadchii, T. Kuzmichev, J.-Y. Lin, S. Kuzmichev, O. Volkova, and A. Vasiliev, CrystEngComm **15**, 1989 (2013).
[32] See Supplemental Material at http://link.aps.org/supplemental/10.1103/PhysRevLett.117.157003 for details on the doping level of samples, the orbital composition of the α pocket, the simulation of the smallest resolvable gap size, the fitting of the superconducting gap and the single-particle scattering rate, some data with a low signal-to-noise ratio, and the superconducting gap distribution on pockets α and ε along k_z.
[33] Y. Zhang, Z. R. Ye, Q. Q. Ge, F. Chen, J. Jiang, M. Xu, B. P. Xie, and D. L. Feng, Nat. Phys. **8**, 371 (2012).
[34] M. D. Watson, T. K. Kim, A. A. Haghighirad, S. F. Blake, N. R. Davies, M. Hoesch, T. Wolf, and A. I. Coldea, Phys. Rev. B **92**, 121108 (2015).
[35] J. Maletz *et al.*, Phys. Rev. B **89**, 220506 (2014).
[36] Y. Suzuki *et al.*, Phys. Rev. B **92**, 205117 (2015).
[37] M. D. Watson, T. K. Kim, L. C. Rhodes, M. Eschrig, M. Hoesch, A. A. Haghighirad, and A. I. Coldea, arXiv:1603.04545.
[38] Y. Zhang *et al.*, Phys. Rev. B **85**, 085121 (2012).
[39] E. Razzoli, G. Drachuck, A. Keren, M. Radovic, N. C. Plumb, J. Chang, Y.-B. Huang, H. Ding, J. Mesot, and M. Shi, Phys. Rev. Lett. **110**, 047004 (2013).
[40] M. R. Norman, M. Randeria, H. Ding, and J. C. Campuzano, Phys. Rev. B **57**, R11093 (1998).
[41] Y. Zhang *et al.*, Phys. Rev. Lett. **105**, 117003 (2010).
[42] S. Mukherjee, A. Kreisel, P. J. Hirschfeld, and B. M. Andersen, Phys. Rev. Lett. **115**, 026402 (2015).
[43] D. J. Scalapino, Rev. Mod. Phys. **84**, 1383 (2012).
[44] J. Hu and H. Ding, Sci. Rep. **2**, 381 (2012).
[45] S. Maiti, R. M. Fernandes, and A. V. Chubukov, Phys. Rev. B **85**, 144527 (2012).
[46] J. Kang, A. F. Kemper, and R. M. Fernandes, Phys. Rev. Lett. **113**, 217001 (2014).
[47] Z. P. Yin, K. Haule, and G. Kotliar, Nat. Phys. **10**, 845 (2014).
[48] X. Lu, C. Fang, W. F. Tsai, Y. Jiang, and J. Hu, Phys. Rev. B **85**, 054505 (2012).
[49] H. Kontani (private communication).